Early Life Stress in Mice Leads to Impaired Colonic Corticosterone Production and Prolonged Inflammation Following Induction of Colitis

Rachel Q. Muir, BS,[*] **Barbara J. Klocke, MS,**[*] **Melissa S. Jennings, BS,**[*] **Patrick A. Molina, PhD,**[†]
Jung-Shan Hsu, MS,[*] **Cailin E. Kellum, BS,**[†] **Katie L. Alexander, PhD,**[†] **Goo Lee, MD,**[*]
Jeremy B. Foote, DVM, PhD,[‡] **Robin G. Lorenz, MD, PhD,**[§] **Jennifer S. Pollock, PhD,**[†] and
Craig L. Maynard, PhD[*,†]

From the [*]Department of Pathology, University of Alabama at Birmingham, Birmingham, AL USA
[†]Department of Medicine, University of Alabama at Birmingham, Birmingham, AL USA
[‡]Department of Microbiology, University of Alabama at Birmingham, Birmingham, AL, USA
[§]Department of Research Pathology, Genentech, San Francisco, CA USA
Address correspondence to: Craig L. Maynard, 1825 University Blvd, SHEL 613, Birmingham, AL 35294 USA, Ph: (205) 996-0136, (craigmaynard@uabmc.edu).

Background: Early life stress (ELS) is an environmental trigger believed to promote increased risk of IBD. Our goal was to identify mechanisms whereby ELS in mice affects susceptibility to and/or severity of gut inflammation.

Methods: We utilized 2 published animal models of ELS. In the first model, newborn mice were separated from the dam daily for 4 to 8 hours starting on postnatal day 2 and then weaned early on postnatal day 17. Control mice were left undisturbed with the dams until weaning on postnatal day 21. In the second model, dams were fed dexamethasone or vehicle ad libitum in drinking water on postpartum days 1 to 14. Plasma and colonic corticosterone were measured in juvenile and adult mice. Colitis was induced in 4-week-old mice via intraperitoneal injection of interleukin (IL)-10 receptor blocking antibody every 5 days for 15 days. Five or 15 days later, colitis scores and transcripts for *Tnf*, glucocorticoid receptors, and steroidogenic enzymes were measured.

Results: Mice exposed to ELS displayed reduced plasma and colonic corticosterone. Control animals showed improvements in indices of inflammation following cessation of interleukin-10 receptor blockade, whereas ELS-exposed animals maintained high levels of *Tnf* and histological signs of colitis. In colitic animals, prior exposure to ELS was associated with significantly lower expression of genes associated with corticosterone synthesis and responsiveness. Finally, TNF stimulation of colonic crypt cells from ELS mice led to increased inhibition of corticosterone synthesis.

Conclusions: Our study identifies impaired local glucocorticoid production and responsiveness as a potential mechanism whereby ELS predisposes to chronic colitis in susceptible hosts.

Lay Summary

Using 2 distinct animal models, this study shows that in mice, early life stress leads to reduced colonic corticosterone and that induction of colitis after stress removal results in reduced transcription of glucocorticoid synthesis genes, increased *Tnf*, and enhanced chronicity of intestinal inflammation.

Introduction

Inflammatory bowel disease (IBD) develops at the intersection of genetic susceptibility and dysregulated immune responses to the microbiota and other environmental triggers. There is still no cure for IBD. However, consistent with the elevated levels of tumor necrosis factor (TNF) in affected tissue of IBD patients and the role of this cytokine as a dominant inflammatory mediator of IBD,[1] some of the most effective therapies for induction of remission are neutralizing antibodies against TNF.[2,3] Environmental triggers of inflammation, including various forms of psychological stress are arguably the least understood contributing factors despite increasing acknowledgment of the potential of these stimuli to impact IBD development and/or relapse. Acute psychological stress has long been acknowledged to exacerbate symptoms and trigger relapses in IBD patients.[4–6] Moreover, epidemiological studies retrospectively identified significant positive correlations between IBD diagnosis and adverse childhood experiences (ACEs)—traumatic experiences that occur prior to adulthood.[7] In 2019, the US Centers for Disease Control and Prevention (CDC) reported that of 100 000 adults studied across 25 states, 1 in 6 had experienced 4 or more types of ACEs and that 5 of the top 10 leading causes of death are associated with ACEs.[8] Considering the rates of diagnosis

Key Messages

What is already known?

Early life stress can lead to reduced hypothalamic-pituitary-adrenal (HPA) axis function and predispose to increased severity of systemic inflammatory disease.

What is new here?

Early life stress inhibits intestinal production of and sensitivity to corticosterone and predisposes to enhanced chronicity of colonic inflammation that is induced after stress exposure.

How can this study help patient care?

Considering the multiple stress signals encountered during the formative years of life, an improved understanding of the mechanisms whereby ELS impacts gut immune regulatory cascades can ultimately enhance our ability to predict and/or manage the effects of ELS in IBD-susceptible individuals.

of IBD in children and adolescents, and the multiple potential stress signals encountered during early life, an improved understanding of the mechanisms whereby ELS impacts gut immune regulation in health and during inflammation can ultimately enhance our ability to predict and/or manage the effects of ELS in IBD-susceptible individuals.

The main stress response system of the body is the hypothalamic-pituitary-adrenal (HPA) axis, and it is known that ELS can lead to HPA-axis dysfunction.[9,10] Upon receipt of a perceived stressor, the paraventricular nucleus of the hypothalamus secretes corticotrophin-releasing factor (CRF) and arginine vasopressin (AVP). Corticotrophin-releasing factor and AVP stimulate the anterior pituitary gland to secrete adrenocorticotropic hormone (ACTH), which then activates the adrenal glands to release glucocorticoids (GCs), cortisol in humans and corticosterone (CORT) in rodents.[10] Glucocorticoids can negatively feedback into the HPA-axis in a dose- and duration-dependent manner to repress the HPA-axis-mediated stress response, including GC production.[11] This controlled regulation of HPA-axis activity is crucial because excessive or diminished GC release can have dire metabolic and immunological consequences.[12,13]

Systemic GCs are derived from adrenal glands and can impact multiple physiological processes,[13,14] but other organs including the intestine are also capable of producing GCs.[15] Intestinal GCs are synthesized by crypt epithelial stem cells following activation of liver receptor homolog-1 (LRH-1), which transcriptionally regulates the expression of steroidogenic enzymes including CYP11A1 and CYP11B1.[16] Glucocorticoids can signal to multiple cell types due to the ubiquitous expression of the GC receptor (GCR, encoded by *Nr3c1*). Under homeostatic conditions, colon-derived GCs promote maturation and preservation of the epithelial barrier and, being potent immune suppressors, help regulate immune cell activation and proliferation.[17,18] Gut-specific GC synthesis has also been implicated in IBD pathogenesis, as transcriptome-wide association studies have identified *NR5A2* (which encodes LRH-1) as a susceptibility gene

for both Crohn's disease (CD) and ulcerative colitis (UC).[19] Compared with healthy tissue, inflamed colonic biopsies from UC and CD patients exhibit significantly lower levels of *NR5A2*, *CYP11A1*, and *CYP11B1*.[20] Owing to their anti-inflammatory capabilities, administration of synthetic GCs is common practice for the treatment of several inflammatory diseases including IBD.[21] Furthermore, therapeutic targeting of colonic GC production successfully impeded experimental IBD; and consequently, investigation into the potential clinical use of LRH-1 agonists is ongoing.[22]

Altogether, current knowledge suggests that downregulation of GC output due to chronic stress can directly and profoundly impact intestinal immune homeostasis and local control of microbiota-dependent inflammation when it arises. Therefore, our goals in this study were to examine (1) whether and how ELS might cause local disruptions in intestinal immune homeostasis, and (2) the potential impact of ELS on the subsequent development and progression of induced colitis. We first employed an established murine model of ELS based on maternal neglect—maternal separation with early weaning (MSEW). In this model, ELS resulted in impaired production of colonic corticosterone and reciprocally skewed expression of anti-inflammatory interleukin (IL)-10 and pro-inflammatory interferon-gamma (IFNγ) by mucosal CD4 T cells. When subjected to induction of chronic colitis via transient blockade of the IL-10 receptor, ELS mice displayed increased chronicity of disease characterized by sustained expression of *Tnf* and damage to the epithelial barrier. In a separate model of ELS involving direct HPA axis disruption via postnatal feeding of the synthetic glucocorticoid dexamethasone (Dex), we observed similarly impaired colonic CORT as in MSEW mice and a similar chronic disease phenotype following introduction of a colitogenic insult. In precolitic ELS mice and despite the lower levels of colonic corticosterone, we observed no differences in expression of *Nr5a2* compared with control animals. However, the chronic phase of colitis was associated with significant downregulation of *Nr5a2* and the Lrh-1 transcriptional target steroidogenesis enzyme *Cyp11a1*. Conversely, colonic crypt cells that are the primary source of colonic CORT harbored increased TNF receptor transcripts. Additionally, TNF stimulation suppressed GC output of colonic crypt cells from ELS mice, more so than cells enriched from control mice. Collectively, our results demonstrate that ELS enhances the inflammatory tone of the intestine and predisposes to further suppression of intestinal GC synthesis during chronic intestinal inflammation.

Materials and Methods

Mice

All mice used in this study were of the C57BL/6 genetic background, originally acquired from Jackson Laboratories (Bar Harbor, ME). In initial studies, we observed substantial variability in stress response phenotypes and disease outcomes in female mice that was not evident in males, reminiscent of our previous findings that MSEW promoted endothelial dysfunction in male but not female mice.[23] Therefore, the results presented herein were generated using male mice. All mice were bred and maintained under specific pathogen-free (SPF) conditions at the University of Alabama at Birmingham in accordance with Institutional Animal Care and Use Committee (IACUC) guidelines.

Maternal Separation With Early Weaning

Maternal separation with early weaning (MSEW) was performed as previously described.[23,24] Briefly, pregnant females were monitored and randomly assigned to either normal rear (NR) or MSEW groups. To minimize "cage effects" on the microbiota, each dam underwent 2 breeding cycles with alternating assignments to NR or MSEW, that is, dams with normally reared control litters in the first breeding round had litters assigned to the MSEW group in the second breeding round and vice versa. Exact day of birth was noted as postnatal day 0 (PD0). Litters with MSEW mice were separated from dams for 4 hours/day on PD2 to PD5 from 9:00 AM to 1:00 PM. From PD6 to PD16, MSEW pups were separated for 8 hours/day from 9:00 AM to 5:00 PM. The MSEW pups were weaned on PD17 with ad libitum access to food and water. During the separation period, pups were housed in an Animal Intensive Care Unit (AICU) incubator (Lyon Technologies, Catalog No. 912-062) at 37.5°C and 60% humidity. Normally reared (NR) litters remained undisturbed with dams until standard weaning on PD21. All mice were maintained on standard chow (NIH-31; NSN 8710-01-005-8438) following weaning. After weaning, females were rested for a minimum of 7 days prior to being mated again.

Dexamethasone Administration

To promote its solubility in water, dexamethasone (D9184, Sigma) was first suspended in vehicle solution composed of 0.002% dimethyl sulfoxide (DMSO, BP231, Thermo Fisher) and 0.02% 2-hydroxypropyl-b-cyclodextrin (H107, Sigma). Dexamethasone was delivered in the drinking water from PD1 to PD14 at a final concentration of 3.0 µg/mL. An equal volume of vehicle solution was diluted in water and provided to control animals. Pregnant females were monitored so that exact day of birth could be noted as PD0. Vehicle or dexamethasone was administered ad libitum in drinking water from PD1 to PD14. Fresh preparations were provided every 5 days, and all cages were returned to normal drinking water on PD14.

Assessment of Intestinal Permeability

Four-week-old mice were fasted for 6 hours then gavaged with fluorescein isothiocyanate (FITC)-conjugated dextran (FITC dextran, Sigma Aldrich) at 400 mg/kg body weight. Four hours after gavage, blood was collected via the retro-orbital plexus into heparinized tubes, and plasma was separated by centrifugation at 10 000 g for 10 minutes at room temperature. Plasma was diluted 1:4 in sterile deionized (DI) water in a 96-well plate. Fluorescence was detected by a Synergy HT spectrophotometer (Biotek; excitation: 485 nm, emission: 528 nm). FITC dextran was dissolved in sterile DI water at final concentrations ranging from 0 to 10 000 ng/mL, which was used to calculate FITC dextran concentrations of the samples. Fluorescent emission signals in the plasma of mice that did not receive FITC dextran were averaged and subtracted from emission signals of mice treated with 4-kDa FITC dextran to eliminate background signal.

Tissue Dissociation and Flow Cytometry

Mesenteric lymph nodes and/or colons were collected from mice between 8:00 AM and 1:00 PM and were mechanically dissociated in RPMI medium; the cell suspension was filtered through a 70-µM mesh strainer. Mesenteric fat was removed from colons, and colons were flushed with sterile phosphate-buffered saline (PBS) and cut open longitudinally. Tissue was sectioned into 1-cm pieces and incubated for 20 minutes at 37°C with rotation in 154 µg/L $_L$-dithioerythritol and 2 µM ethylenediaminetetraacetic acid (EDTA) in Hank's balanced salt solution (HBSS) to remove the mucus and epithelial cells. The tissue was then incubated at 37°C with rotation in 20 µg/mL DNase-I and 100 U/mL collagenase 4 (Sigma-Aldrich), and tissue digestion was completed with a GentleMACS Dissociator (Miltenyi Biotec). Lamina propria cells were further purified on a 35% percoll gradient with room temperature centrifugation for 20 minutes at 500 × g with no brake. Cells were washed with PBS, blocked with 2.4G2 (BioXCell, 10 µg/mL), and then stained with LIVE/DEAD Fixable Near-IR (Invitrogen) and antimouse antibodies purchased from BioLegend: CD4 (GK1.5), TCRβ chain (H57-597), IL-17A (TC11-18H10.1), CD90.1 (OX-7), or eBioscience, Foxp3 (FJK-16S), and IFNγ (XMG1.2). Cells for effector cytokine staining were stimulated at 37° in RPMI medium with 10% fetal bovine serum (FBS) (R10 medium) with ionomycin (750 ng/mL), phorbol 12-myristate 13-acetate (50 ng/mL), and GolgiPlug (BD Biosciences). Intracellular staining was performed after cell permeabilization using the Foxp3/Transcription Factor Fixation/Permeabilization Kit (eBioscience). All cells were fixed in 2% paraformaldehyde and acquired with an LSR 2 cytometer (BD Biosciences). Data were analyzed using FlowJo software (TreeStar).

Interleukin-10 Receptor Neutralization

Following the end of the ELS-inductive period, 4-week-old mice were injected intraperitoneally with 100 µg of anti-IL-10R (BE0050, BioXCell) or vehicle (PBS; 21-040-CV, Corning) every 5 days for 15 days. Injections were administered between 2:00 and 4:00 PM. Mice were killed on day 20 or 30 after the initial anti-IL-10R injection.

Assessment of Colitis

Representative sections of the proximal, middle, and distal colon were fixed in 2% buffered formalin then embedded in paraffin. 5 um sections were cut and stained with hematoxylin and eosin (H&E). Histological scoring was performed using a previously established scheme[25] from a veterinary pathologist who was blinded to the experimental groups. Representative images were collected using Nikon Eclipse Ci microscope and analyzed with NIS-Elements software.

Measurement of CORT, ACTH, and TNF

Blood was collected either by retro-orbital bleeding from isoflurane anesthetized mice or via cardiac puncture at necropsy, all between 8:00 AM and 1:00 PM. Plasma was separated by centrifugation at 3630 g for 10 minutes at 4°C and stored at –80°C until use. Colonic tissue was rinsed and voided of fecal contents, cut into 1-cm pieces, and incubated at 37°C and 5% CO_2 in 500 µL R10 medium in a 48-well plate. After 48 hours, contents of each well were transferred to a 1.5-mL tube and centrifuged at 20 000 g for 8 minutes; the colon culture supernatant was collected and stored at –80°C until use. Corticosterone levels were detected using

the DetectX Corticosterone Enzyme Immunoassay Kit (K014-H5, Arbor Assays). Plasma ACTH levels were detected using the ACTH Enzyme Immunoassay Kit (EIA-ACTH-5, RayBiotech). Tumor necrosis factor levels were detected using the Mouse TNF-alpha DuoSet ELISA kit (DY410-05, R&D Systems). Total protein was determined via the bicinchoninic acid (BCA) protein assay from colon culture supernatant samples.[26] Colon culture corticosterone levels were normalized to total protein.

Real-time Polymerase Chain Reaction

Proximal colonic tissues were homogenized using the Omni tissue homogenizer (Omni International, TH115). Total RNA was extracted from whole colonic tissue or from enriched epithelial cells using TRI Reagent (Zymo Research, R2050-1-200). For colon crypt-enriched epithelial cells, total RNA was extracted using the E.Z.N.A Total RNA Kit 1 (Omega Bio-Tek, R6834-02). Reverse transcription polymerase chain reaction (PCR) was performed using a C1000 Touch Thermal Cycler (Bio-Rad) with a High-Capacity cDNA Reverse Transcription Kit (Thermo Fisher Scientific, 4368813). Real time quantitative PCR was performed on a QuantStudio 3 system (Thermo Fisher Scientific) with SsoAdvanced Universal SYBR Green Supermix (Bio-Rad, 1725274). Gene expression was normalized to TATA box-binding protein mRNA. Primer sequences can be seen in supplementary data (Table S1).

Isolation and Stimulation of Colonic Crypt Cells

Mesenteric fat was removed from the colon prior to flushing luminal contents with PBS. The proximal colonic tissue was cut into 0.2-cm pieces and washed 3 times via serological pipetting with 10 mL of cold Dulbecco's PBS (DPBS) (MT21031CM, Corning). Tissue pieces were settled by gravity and the supernatant was vacuum aspirated. To release crypt epithelial cells, tissue was digested 3 times for 20 minutes at 37°C with rotation in collagenase type 1 (2mg/m1; 17-100-017, Corning). The collagenase was neutralized with DPBS containing 0.1% bovine serum albumin (BSA; BP1600-100, Fisher), and the supernatant containing released epithelial cells was filtered through a 70-μm strainer. The filtered epithelial cell fraction collected after the third digestion step was centrifuged at 290 g for 5 minutes at 8°C, and 1000 cells were suspended in Matrigel (CLS356235, Corning) and plated in a 48-well plate. Cells were cultured with media consisting of 50% L-WRN conditioned media,[71] 50% advanced Dulbecco's modified Eagle's medium (DMEM/F-12; D6421, Sigma), supplemented with 20% fetal bovine serum (SH30109.03, Cytiva), 50 μg/mL of gentamicin (G1397, Sigma), 10 μM of SB 431542, 10 μM of Y-27632, 2.5 μg/mL of fungizone, 100 units/mL of penicillin, and 0.1 of mg/mL streptomycin (16-141-0, 12-541-0, MT30003CF, MT30002CI, Thermo Fisher Scientific). Some wells were stimulated with 10 ng/mL TNF (T7539, Sigma). Culture supernatants were collected after 48 hours.

Statistical Analysis

Statistical significance was calculated by unpaired Student t test, Mann-Whitney U test, 1-way ANOVA, 2-way ANOVA, or Brown-Forsythe test as appropriate, using Prism software (GraphPad). All $P \leq .05$ values are considered significant and indicated as such in the text.

Results

ELS in Mice Disrupts Systemic and Colonic Glucocorticoid Production

For our initial studies, we used the maternal separation with early weaning model of ELS, designed to mimic maternal neglect during the suckling period.[24] In this model, newborn pups are separated from the moms daily during the resting period (Figure 1A). On day of life (DOL) 2 to 5, pups were separated for 4 hours daily and then from DOL 6 to 16 for 8 hours daily. Mice were then weaned on DOL 17, 4 days before their normal rear (NR) counterparts—who were never separated from the moms—were weaned on DOL 21. These experiments were also conducted using our previously developed IL-10 reporter (10BiT) mice[27] to allow simultaneous analysis of IL-10–producing cell subsets known to be critical for the establishment and maintenance of intestinal immune homeostasis. It has been reported that various models of stress including MSEW can result in increased intestinal permeability.[28] In our hands, on DOL 28, we saw no difference in basal permeability between NR and MSEW mice (Figure 1B). However, relative to normally reared mice, MSEW mice had significantly lower levels of circulating CORT but surprisingly, no difference in ACTH (Figure 1, C-D). Significantly lower CORT was also detected in supernatants collected after colon tissue from MSEW mice were cultured ex vivo without any additional stimulation (Figure 1E). These data argue that ELS can directly impair GC synthesis by both adrenal glands and colonic stem cells independent of any effects on corticosterone-inducing ACTH.

Transient Decrease in IL-10-producing T cells, Followed by Increased IFNγ+ T cells in Mesenteric Lymph Nodes of MSEW Mice

We assessed live CD4+ T cells of the mesenteric lymph nodes (MLNs) at 4 and 8 weeks of age in NR and MSEW mice to evaluate the impact of ELS on mucosal T cell-dependent immune regulation. There was no difference in the frequency or numbers of Foxp3+ + CD4+ T cells between NR and MSEW mice at either 4 or 8 weeks of age, indicating that MSEW does not impact basal accumulation of MLN Foxp3+ T regulatory (Treg) cells (Figure 1, F-G). Because we utilized the 10BiT mouse line, we were also able to assess IL-10-producing cells based on surface expression of Thy1.1. Interestingly, we found lower frequencies and numbers of IL-10-producing CD4+ T cells at 4 weeks of age in MLNs of MSEW mice relative to NR mice. This difference was no longer present at 8 weeks of age (Figure 1, F, H). Conversely, despite similar frequencies and numbers of interferon gamma (IFNγ)-producing CD4 T cells at 4 weeks of age, we observed significantly greater frequencies and numbers of this population in the MLNs of 8-week-old MSEW mice relative to NR counterparts (Figure 1, 1-J). Collectively, these results indicate that MSEW causes delayed differentiation and/or accumulation of mucosal IL-10–producing cells, which can enable the emergence of pro-inflammatory Th1 effector cells, thereby altering the mucosal immune cell balance.

MSEW Predisposes to Sustained Intestinal Inflammation Following a Colitogenic Insult

To study the effect of ELS on IBD susceptibility and severity, we employed a murine model of colitis predicated on transient
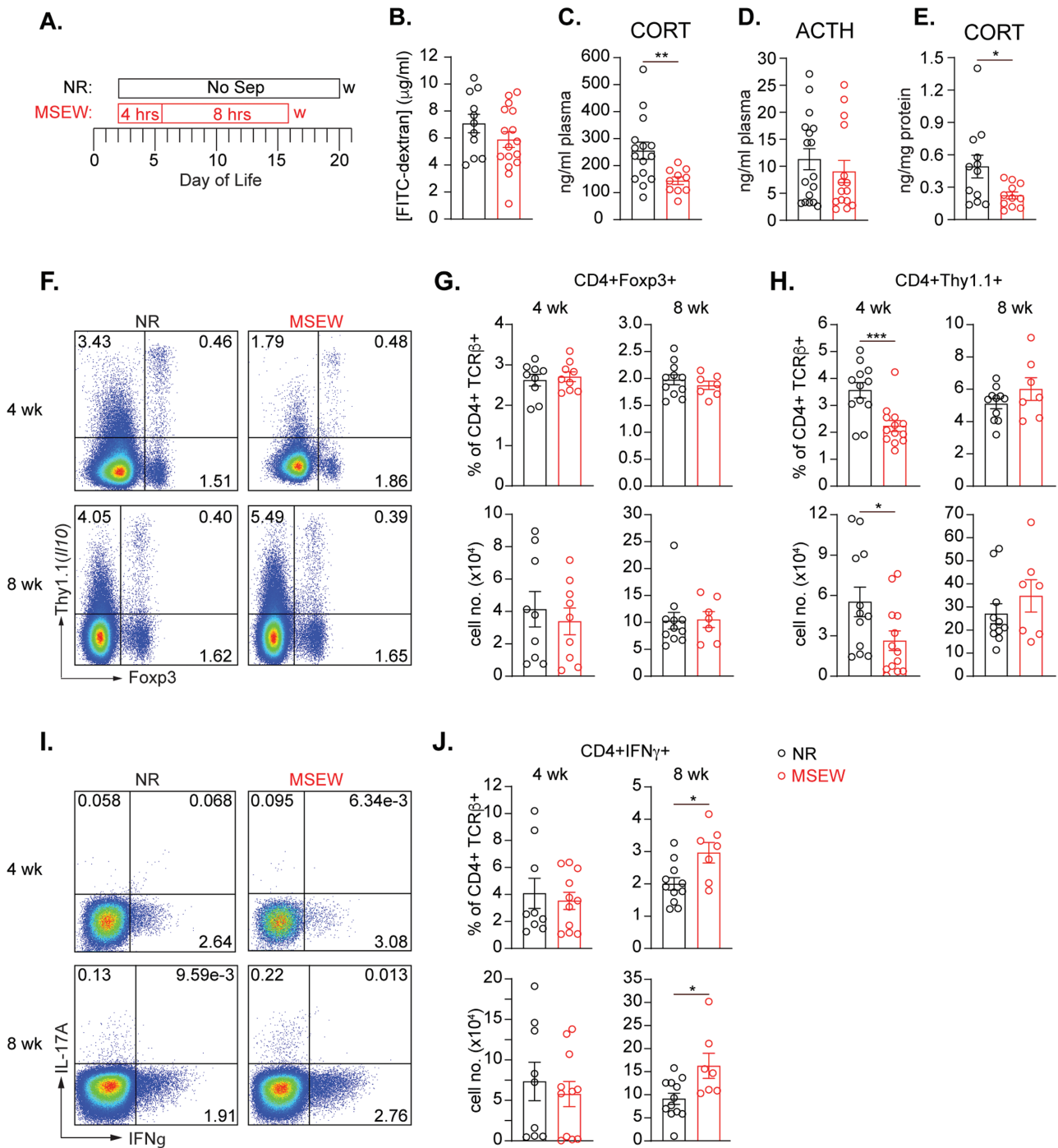
Figure 1. ELS in mice leads to reduced levels of corticosterone and skewed expression of IL-10 and IFNγ by gut-associated CD4 T cells. A, Experimental design for maternal separation with early weaning (MSEW). B, Concentration of FITC-dextran in plasma of 4-week-old mice 4 hours after oral gavage and normalized to plasma from mice that did not receive FITC-dextran. Graphs (C-E) showing plasma concentrations of (C) CORT and (D; ACTH) in 4-week-old NR and MSEW mice as measured by ELISA ($n \geq 10$ mice/grp). E, CORT concentration in supernatants from 48-hour colon cultures of 4-week-old NR and MSEW mice ($n = 11$ mice/grp). F, Representative flow cytometry plots showing Foxp3 and Thy1.1 expression by live CD4 T cells in the MLNs of NR and MSEW mice at 4 (upper), and 8 (lower) weeks of age. Graphs summarizing frequencies (upper) and numbers (lower) of live CD4$^+$Foxp3$^+$ (G) and live CD4$^+$Thy1.1$^+$ (H) determined as in E. I, Representative flow cytometry plots showing IFNγ and IL-17A expression by live CD4 T cells in the MLNs of NR and MSEW mice at 4 (upper) and 8 (lower) weeks of age. I, Frequency (upper) and numbers (lower) of live IFNγ$^+$CD4$^+$T cells determined as in H. Error bars represent mean ± SEM. Asterisks denote significance according to Mann-Whitney U test (B-D) or Student's t test (E-J) at $P < .05$ (*), $P < .01$ (**), and $P < .001$ (***). Data are compiled from 2-3 independent experiments.

disruption of IL-10 receptor (IL-10R) signaling. In this model, antibody blockade of the IL-10R results in mild-moderate colonic inflammation that resolves spontaneously following cessation of antibody treatment. Four-week-old NR and MSEW mice received intraperitoneal injections of anti-IL-10R antibody or vehicle (PBS) every 5 days for 15 days (Figure 2A). Overall, MSEW mice gained weight more rapidly over the course of the experiment than did NR mice (Figure 2B). Mice
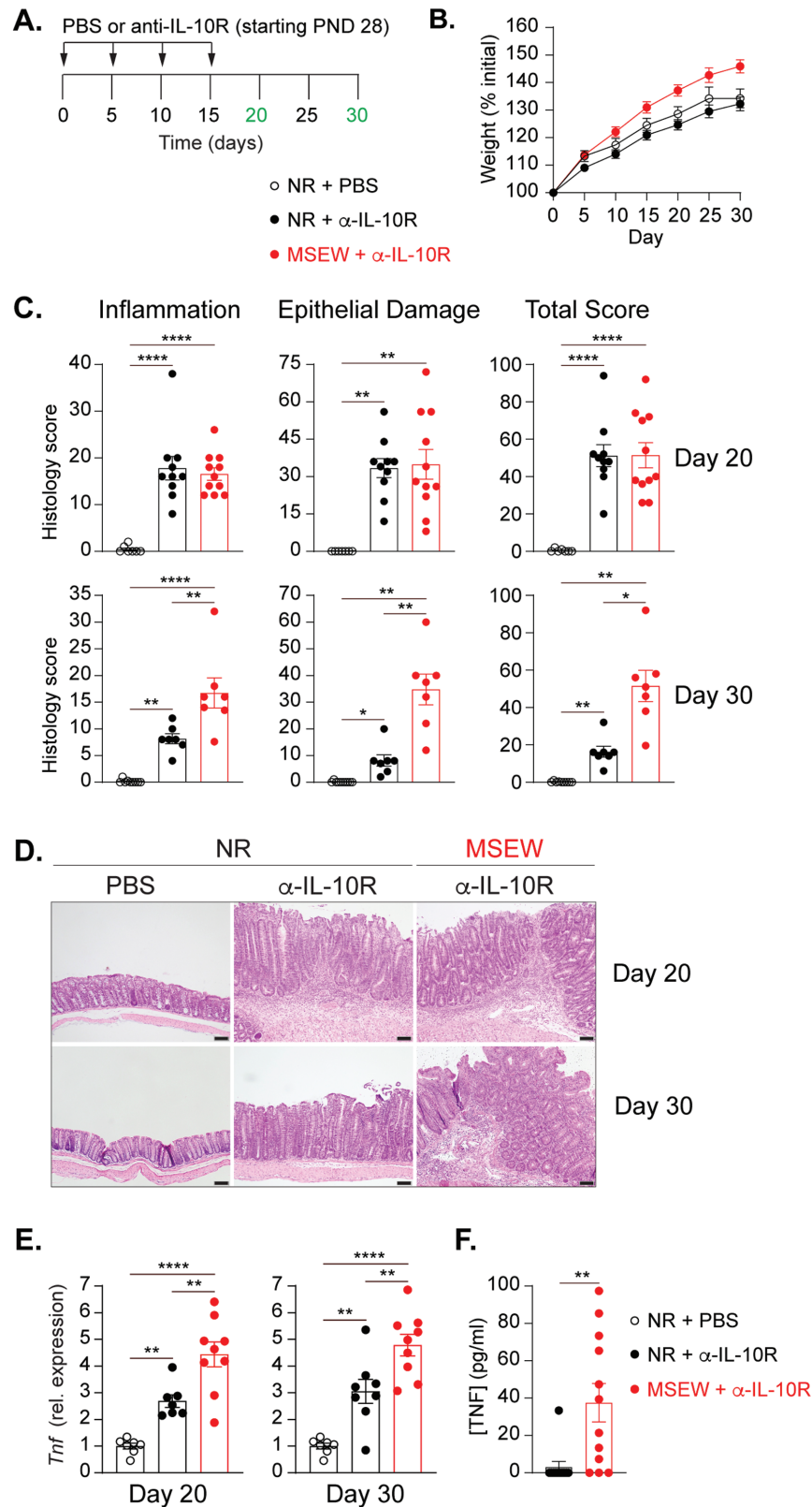
Figure 2. Blockade of the IL-10 receptor subsequent to ELS results in sustained colitis characterized by elevated *Tnf*. A, Experimental design for colitis induction. B, Weight change as a percentage of initial (PND 28) weight over the course of the experiment. C, Graphs showing scores for inflammation, epithelial damage, and total colitis of the proximal colon in PBS- or α-IL-10R–treated NR and MSEW male mice at day 20 and day 30. (n ≥ 7). D, Representative hematoxylin and eosin (H&E) stained colonic tissue sections from PBS- and α-IL-10R–treated NR and MSEW mice. Scale bars = 100μm. E, Relative *Tnf* transcript levels on Day 20 (left), and Day 30 (right) in the proximal colons of NR and MSEW mice treated or not as indicated (n ≥ 7). All transcripts were initially normalized to TATA box binding protein (*Tbp*). F, TNF concentration in supernatants from 48-hour colon cultures of α-IL-10R–treated NR and MSEW mice on Day 20 (n ≥ 7). Error bars represent mean ± SEM. Asterisks denote significance from 1-way ANOVA (C, E) followed by Tukey's multiple comparisons test or unpaired *t* test with Welch's correction (F) at *P < .05, **P < .01, ***P < .001, and ****P < .0001.

were killed 5 and 15 days after the final α-IL-10R injection, that is, days 20 and 30, respectively, after the initiation of IL-10R blockade. As expected, by day 20, there were clear signs of inflammation and epithelial damage that contributed to an overall colitis score that was not different between NR and MSEW mice (Figure 2, C-D, upper panels). However, by day 30, and in contrast to significant resolution of colitis in NR mice, MSEW tissue still displayed visible signs of inflammation, epithelial damage, and an overall colitis that was virtually unchanged from day 20 (Figure 2, C-D, lower panels). Flow cytometric analysis of IFNγ-, IL-17A-, and Foxp3-expressing colonic CD4 T cells revealed that all these subsets were elevated in response to anti-IL-10R treatment, but there were no significant differences in frequency or number between NR and MSEW animals (Figure S1). We also did not detect significant differences in transcript levels of pro-inflammatory Il6, Il1b, or Nos2 (Figure S2). However, as early as day 20, there were already significant differences in Tnf transcript in colonic tissue from MSEW relative to NR animals, and this difference persisted through day 30 (Figure 2E). As confirmation, we detected significantly higher TNF protein levels following ex vivo culture of colon tissue from colitic MSEW mice relative to colitic NR mice (Figure 2F). Much of this transcript difference appeared to be attributable to nonepithelial cells because we observed small but significant differences in Tnf transcript expression among gut tissues crudely denuded of intestinal epithelial cells (IECs) but not among enriched IEC (Figure S3). To determine whether CD4 T cells are responsible for the TNF difference, we performed intracellular staining for TNF in live lamina propria CD4 T cells. Unfortunately, we also did not detect significant differences in the frequencies or numbers of CD4 + TNF + cells, neither were there consistent differences in mean fluorescence intensity of TNF (Figure S3, B and C). Altogether, these results support a role for ELS in enhancing individual susceptibility to chronic gut inflammation characterized by sustained production of TNF, potentially by multiple cell subsets.

ELS Induced by Early Postnatal Glucocorticoid Exposure Recapitulates the Effects of MSEW

The foregoing results suggest a link between ELS-induced reductions in systemic and local GC synthesis. Previous studies associate HPA axis dysfunction with an initial spike in the circulating levels of stress-related hormones followed by a persistent decrease in basal corticosterone release.[29,30] A recent study using maternal feeding of the synthetic GC dexamethasone (Dex) during the postnatal period as a model of ELS corroborates the theory that excessive GCs in the early postnatal phase can lead to impaired output of corticosterone later in life.[31] Therefore, we asked whether early postnatal introduction of glucocorticoids can mimic the effects of MSEW. Timed pregnant females were randomly assigned to control or ELS groups and fed Dex or vehicle (Veh) in drinking water from the day after delivery (postnatal day 1, PND 1) until PND 14. All cages were returned to regular drinking water immediately thereafter, and progeny were weaned as normally done on PND 21 (Figure 3A). As with the MSEW model, we also observed no effect of Dex on basal colonic permeability at 4 weeks of age (Figure 3B). However, there were significantly lower levels of plasma CORT, but not ACTH, in Dex mice relative to Veh controls (Figure 3, C-D). We then examined whether Dex also predisposed to chronic colitis using the

IL-10R blockade model where Dex or Veh mice were injected intraperitoneally with PBS or anti-IL-10R antibody every 5 days for 15 days (Figure 3E). Similar to MSEW mice, Dex mice also gained weight more rapidly during the experimental period (Figure 3F). We observed significant differences in the extent of colon epithelial damage and overall disease severity in Dex mice compared with Veh mice (Figure 3G), similar to MSEW mice. Specifically, colons from Veh mice showed an inflammatory infiltrate limited to the lamina propria and mild crypt epithelial hyperplasia, whereas colons from Dex mice had significantly increased inflammatory infiltrate and epithelial erosion (Figure 3H). Furthermore, like the MSEW model, we did not observe significant differences in transcripts of Il6 or Il1b, their respective receptors, or Nos2 (Figure S3). However, Dex-treated mice displayed elevated Tnf mRNA 30 days postinitiation of anti-IL-10R injections (Figure 3I). Importantly, this was accompanied by increased transcripts of Tnfrsf1a and Tnfrsf1b (which encode TNF receptors 1 and 2, respectively) in crypt-enriched colonic epithelial cells (Figure 3J). Collectively, these data demonstrate that increased GCs in the early postnatal period impairs GC output and can contribute to enhanced severity and chronicity of any inflammation that subsequently develops in the colon. Moreover, this chronic inflammation is accompanied by increased Tnf transcription and seemingly elevated TNF responsiveness by CORT-producing colonic cells.

ELS Leads to Reduced Colonic CORT Levels at Steady State Without Suppression of Nr5a2

The effects of ELS extend well into adulthood, as has been demonstrated in both humans and animal models. Our results demonstrating the effects of 2 different models of ELS on systemic and colonic GC production shortly after cessation of stress exposure (4 weeks of age) raised the possibility of a mechanistic link between the impaired GC synthesis and the colitis observed. Furthermore, given similar outcomes observed in mice subjected to MSEW or maternally transmitted Dex, we conducted side-by-side examination of the effects of both regimens on colonic GC synthesis in the absence of any additional perturbations. In 8-week-old adult mice previously subjected to either MSEW or Dex, colonic corticosterone levels were consistently and significantly lower than that of their control counterparts (Figure 4A). However, we found no differences between mice from either ELS cohort or their control counterparts in the colonic transcripts of the GC receptor Nr3c1 (Figure 4B), suggesting that any downstream effects of reduced GC under these "homeostatic" conditions may not be due to reduced potential for ligand-receptor interactions. We also found no differences in colonic expression of Nr5a2 (which encodes Lrh-1), suggesting the differences in colonic corticosterone at steady state are also not regulated at the level of Lrh-1 expression (Figure 4C).

ELS and TNF Additively Suppress Colonic CORT Output

We then sought to determine the potential effects of ELS on GC synthesis and responsiveness under inflammatory conditions by comparing colonic tissues of colitic MSEW and Dex mice normalized to unstressed, noncolitic animals. We found that overall, inflammation caused modest reductions in Nr3c1 in both stressed and unstressed mice (Figure 4D). However, this decrease was even more pronounced and
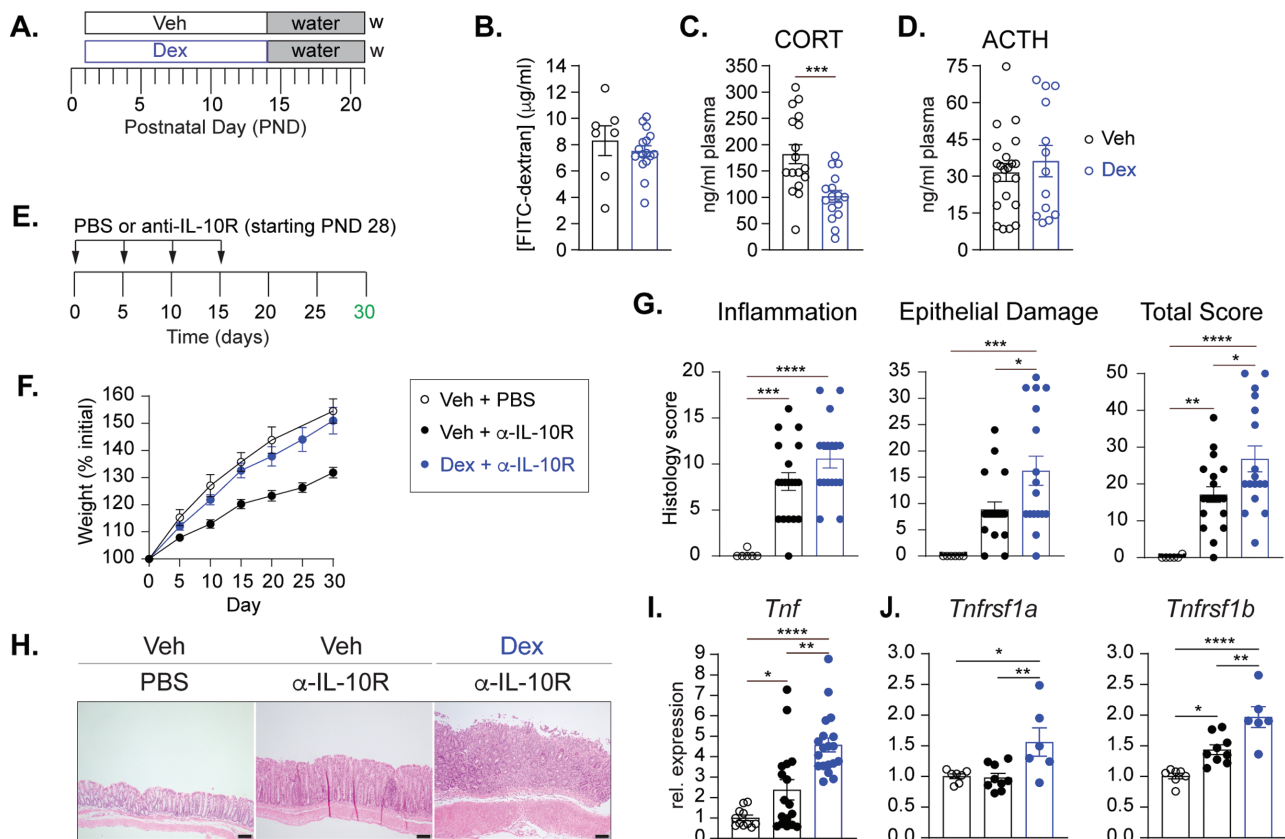
Figure 3. Early postnatal exposure to glucocorticoids recapitulates the effects of MSEW on adolescent mice. A, Experimental design for early life exposure (day of life 1 to 14) to dexamethasone (Dex) or the vehicle (Veh, 0.002% DMSO, 0.02% 2-hydroxypropyl-β- cyclodextrin). B, Concentration of FITC-dextran in plasma of 4-week-old mice 4 hours after oral gavage and normalized to plasma from mice that did not receive FITC-dextran. Graphs (C-D) showing plasma concentrations of (C) CORT and (D; ACTH) in 4-week-old Veh and Dex mice as measured by ELISA ($n ≥ 13$). E, Experimental design for colitis induction, beginning at 4-wks of age, 2-wks post Dex exposure. F, Weight change as a percentage of initial (PND 28) weight over the course of the experiment. G, Graphs showing scores for inflammation, epithelial damage, and total colitis of the proximal colon in α-IL-10R–treated Veh and Dex mice on day 30. ($n ≥ 17$). H, Representative H&E-stained colonic tissue sections from PBS- and α-IL-10R–treated Veh and Dex mice Scale bars = 100µm. I, Relative *Tnf* mRNA levels in proximal colons of α-IL-10R–treated Veh and Dex mice normalized to PBS-treated Veh mice ($n ≥ 10$ mice/group). J, Relative mRNA levels of *Tnfrsf1a* (left) and *Tnfrsf1b* (right) in crypt-enriched epithelial cells from the colons of α-IL-10R–treated Veh and Dex mice, normalized to PBS-treated Veh mice ($n ≥ 6$). All transcripts were initially normalized to *Tbp*. Error bars represent mean ± SEM. Asterisk denotes significant difference from Mann-Whitney U test (C), or 1-way ANOVA followed by Tukey's multiple comparisons test (G, I, J) at *$P < .05$, **$P < .01$, ***$P < .001$, and ****$P < .0001$. Data are compiled from 3 individual experiments.

significantly different in colitic Dex mice relative to Veh-exposed counterparts (Figure 4D, lower). A similar trend was seen in the transcript levels of *Nr5a2*, where inflammation promoted lower expression in both models with a clearly significant difference observed between Dex and Veh mice (Figure 4E). When we examined the expression of the *Nr5a2* transcriptional target *Cyp11a1*, we found that inflammation was associated with a significant upregulation in transcript levels of *Cyp11a1* in colitic but unstressed mice. However, this upregulation was either tempered or completely inhibited in colitic MSEW and Dex mice, respectively (Figure 4F). These findings suggest that ELS has the potential to modulate intestinal GC synthesis pathway, especially in mice subjected to Dex during the suckling period. This was not surprising given that this approach involves more direct and controlled manipulation of the early GC spike believed to be associated with ELS. We thus focused our remaining experiments on mice exposed to vehicle or Dex. In addition to the sustained deficit in local CORT production at steady state that was found in both ELS models (Figure 4A), we also confirmed that there is diminished intestinal CORT output

during active colitis from Dex mice relative to Veh (Figure 4G), providing further support for impaired steroidogenic pathway induction in colitic ELS animals. We next asked whether TNF—the most reproducibly upregulated inflammatory mediator detected in our experiments—was central to the inflammation-induced downregulation of GC synthesis. Indeed, a role for TNF in suppression of colonic GC synthesis has been described.[32] We isolated colonic crypt cells from healthy Veh and Dex mice and cultured in vitro supported by stem cell survival factors in the presence or absence of exogenous TNF. Like the cultures of whole colon tissue (Figure 4A), unstimulated crypt cells from Dex mice spontaneously secreted lower levels of corticosterone than cells from Veh mice. Addition of TNF inhibited the production of corticosterone in both circumstances; but importantly, there was a more significant reduction in expression of corticosterone production by cells from Dex-exposed mice (Figure 4H). Collectively, these data demonstrate that TNF-driven local inflammation potently suppresses colonic GC synthesis and that this effect is further exacerbated by prior exposure to ELS.
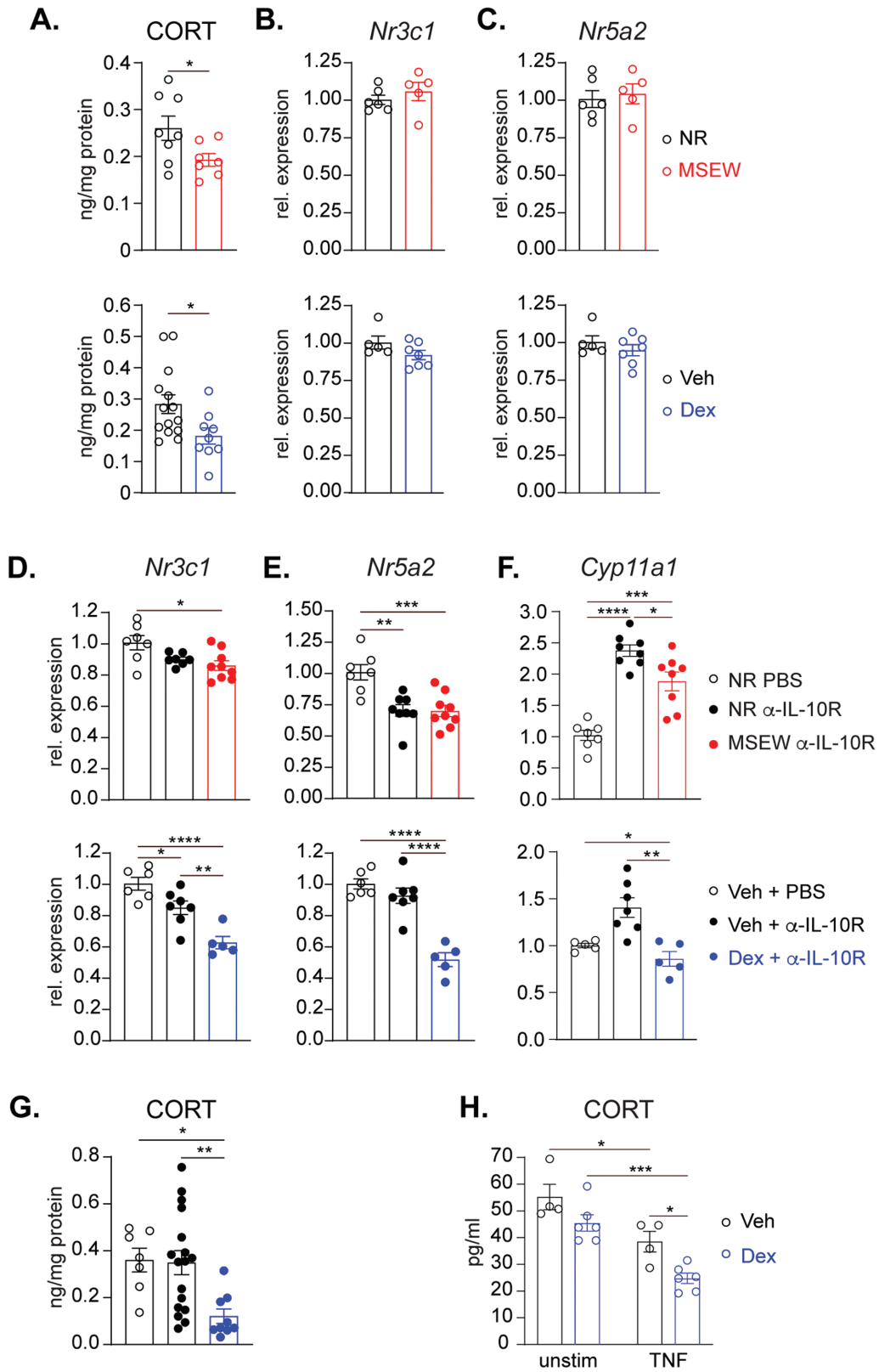
Figure 4. ELS and TNF suppress colonic CORT output. A, Corticosterone concentration in supernatant after 48-hour cultures of colon from 8-week-old NR and MSEW (upper); and Veh and Dex mice (lower; $n \geq 7$). B, Relative expression of *Nr3c1* and (C) *Nr5a2* in proximal colons of healthy NR versus MSEW (upper) and Veh versus Dex (lower) mice ($n \geq 5$). D-F, Relative expression of (D) *Nr3c1*, (E) *Nr5a2*, and (F) *Cyp11a1*, in proximal colons of α-IL-10R–treated NR and MSEW mice (upper), and Veh and Dex mice (lower), normalized to PBS-treated NR and Veh mice, respectively ($n \geq 7$). All transcripts were initially normalized to *Tbp*. G, Corticosterone concentration in supernatant after 48-hour cultures of colon from 8-week-old α-IL-10R–treated Veh and Dex mice at Day 30 ($n \geq 9$). H, Corticosterone concentration as determined by ELISA in supernatant of proximal colonic crypt cells generated from 8-week-old Veh and Dex mice stimulated or not with 10 ng/mL TNF stimulation for 48-hour ($n \geq 4$). Error bars represent mean ± SEM. Asterisks denote significant differences from Student's t test at (A), 1-way (D-G) or 2-way (H) ANOVA followed by Tukey's multiple comparisons test at *$P < .05$, **$P < .01$, ***$P < .001$, and ****$P < .0001$.

Discussion

In this study, we examined the effects of ELS on mediators of intestinal immune regulation and on the chronic phase of colonic inflammation induced secondarily to ELS. As validation of our approach, we showed that whether induced via MSEW or postnatal dexamethasone exposure, ELS resulted in HPA axis dysfunction, evidenced by reduced circulating levels of CORT. In addition, we demonstrate for the first time that ELS also leads to impaired production of CORT in the colon both in the adolescent period shortly after removal of the stress signal and in adulthood. This reduced local CORT may be central to the increased inflammatory tone of the intestine, which was characterized by early deficits in mucosal IL-10–producing CD4 T cells followed by increased IFNγ-producing CD4 T cells in early adulthood. Although ELS has been reported to alter intestinal barrier integrity and promote low-grade inflammation in mice,[28,33–36] in noncolitic MSEW and Dex mice, we did not detect differences in basal epithelial permeability or any overt pathology relative to control mice. Manifestation of the effects of ELS on gut inflammation required the introduction of a colitogenic insult for which we employed antibody-mediated blockade of the IL-10 receptor. Thus, our study demonstrates how this environmental trigger can induce and imprint disruptions in normal gut immune homeostasis and can have long-term effects on the predisposition to and perpetuation of chronic inflammation in susceptible hosts (Figure 5).

The literature reports contradictory effects of ELS on circulating GC concentrations in both humans and laboratory animals with GCs elevated in some settings[37,38] and decreased in others.[39–41] The change in CORT is often directly related to changes in the levels of circulating ACTH, the primary
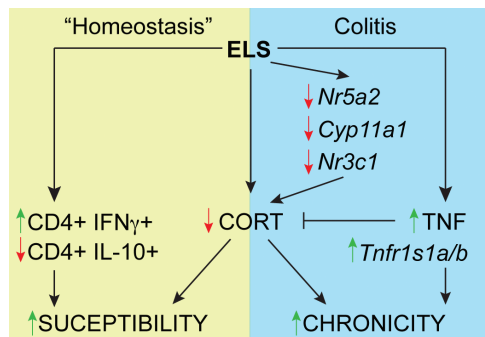

Figure 5. Proposed model of the impact of ELS in health and disease. ELS results in reduced production of colonic corticosterone (CORT). In otherwise healthy ELS mice under "homeostatic" conditions, ELS also alters the mucosa-associated immune cell balance with an initial deficit in anti-inflammatory IL-10-producing CD4 T cells followed by an increase in IFNγ-producing CD4 T cells. This diminished local CORT and altered mucosal immune milieu enhance the susceptibility of ELS-exposed individuals to inflammation especially in the presence of additional colitogenic insults. During active colitis, local deficits in CORT production and function are further reinforced via reductions in (1) *Nr5a2*, the gene encoding Lrh1 that is responsible for colonic CORT production, (2) *Cyp11a1*, which encodes the first enzyme involved in de novo steroidogenesis, and (3) *Nr3c1*, which encodes the global GCR. Conversely, colitis in ELS animals is consistently associated with (1) increased intestinal TNF production, which can further suppress local CORT synthesis, and (2) increased transcription of genes encoding TNF receptors 1 and 2. The combination of increased TNF and reduced CORT contributes to a sustained inflammation in the colons of ELS-exposed mice.

activator of CORT release by adrenal glands. Despite the reduced CORT, in both models of ELS, we did not detect significant changes in circulating ACTH. Yet, although we did not directly assess adrenal gland CORT secretion, impaired adrenal gland GC output in response to stress is the most likely reason for the reduced plasma CORT levels in our ELS mice. Notably, in the absence of inflammation in the intestine, we also did not detect changes in expression of *Nr5a2*, the gene encoding Lrh-1 that transcriptionally regulates colonic CORT synthesis. Thus, both models of ELS resulted in lower basal levels of adrenal- and intestinal-derived CORT without affecting expression of the established upstream mediators of GC synthesis and/or release.

In contrast to the otherwise steady state, under inflammatory conditions we detected ELS-dependent reductions in expression of *Nr5a2* and *Cyp11a1,*and a corresponding significant decrease in intestinal CORT output from colitic ELS mice relative to colitic unstressed mice. Our findings are consistent with the reported downregulation of *NR5A2* in the colons of ulcerative colitis patients.[42] Colon tissue from colitic ELS mice also showed lower expression of *Nr3c1*, the gene encoding the GCR. Thus during inflammation, prior exposure to ELS contributes to reduced CORT output and signaling, which collectively can contribute to the chronicity of colitis via inadequate control of pro-inflammatory mediators. Interestingly, all these transcripts were altered in unstressed mice with colitis, demonstrating effects of inflammation independent of ELS. However, particularly in colitic Dex mice, each was more substantially altered/downregulated, suggesting additive effects of ELS and inflammation. The reason for the discordance in GC receptor transcripts in control vs ELS colons during health and disease is currently unclear. Further studies will be required to delineate the potentially distinct mechanisms underlying ELS-mediated suppression of CORT synthesis and sensitivity in the colon under the 2 conditions.

Chronic inflammation in mice is characterized by upregulation of numerous pro-inflammatory pathways in both innate and adaptive immune effector cells. Accordingly, we found that independent of ELS, there was elevated Th1 and Th17 cells and increased mRNA of pro-inflammatory cytokines IL-1β and IL-6 in colonic tissue of colitic mice. However, across multiple experiments in 2 different models, *Tnf* was the only factor examined for which we consistently detected significantly higher transcript levels in ELS mice relative to control mice. We were unable to identify a single cell population that is primarily responsible for the elevated Tnf in ELS mice. At a minimum, our data appears to exclude epithelial cells and potentially CD4 T cells as being solely responsible. Thus, we speculate that the elevated TNF may be a net effect of moderate overproduction by multiple cell types in the lamina propria. Our results also suggest that expression of the GCR is a major feature of the culpable cell type(s), and the near ubiquitous expression of the GCR further supports the notion that multiple cellular sources of TNF may be involved.

Despite not identifying a primary source of TNF, our results suggest that CORT-producing colonic crypt stem cells are important targets of TNF in colitic ELS mice. Specifically, crypt-enriched colonic epithelial cells harbored increased transcripts of the genes encoding TNF receptors 1 and 2—but not those encoding IL-1 or IL-6 receptors—and produced less CORT in the presence of TNF. This led us to explore the potential intersection of TNF and local

colonic CORT in mediating the long-term effects of ELS in colitic mice. Even prior to our study, it was known that this is a complex relationship. For example, in acute colitis in mice, TNF administration can trigger CORT synthesis to reduce disease.[43] Conversely, in chronic colitis, TNF can prevent CORT synthesis via suppression of *Nr5a2*, and TNF blockade can restore intestinal CORT synthesis to limit disease activity.[44] Interestingly in the same study, lower amounts of TNF over a shorter duration induced expression of intestinal steroidogenic genes, suggestive of a dose-dependent relationship.[44] In our study, we found that the ELS-induced deficit in colonic CORT existed under "homeostatic" conditions when TNF levels were minimal or undetectable and persisted well into the chronic phase of colitis, which was characterized by constantly elevated TNF. Furthermore, in vitro stimulation of colonic crypt cells with high-dose TNF—used to mimic severe chronic inflammation—resulted in significantly reduced CORT output, especially in cells from Dex-exposed mice. This inhibition of CORT synthesis by TNF is likely self-perpetuating. Both the GCR and TNF can be expressed by multiple intestinal cell types during inflammation, meaning that inadequate CORT signaling to any or all the major TNF-producing subsets can result in failure to regulate TNF production and potentially sustain the inflammatory reaction. Thus, our study supports a model wherein ELS predisposes to prolonged colitis via insufficient local production of CORT via direct targeting of crypt stem cells by TNF coupled with reduced GCR availability, enabling additional TNF production and signaling.

The exact molecular pathway whereby ELS targets and imprints colonic crypt cells also remains to be elucidated. Studies in humans and rodents have uncovered ELS-induced epigenetic alterations in multiple stress-response genes across various regions of the brain.[45,46] These changes have been found to impact GC output and alter the functional signaling capability of the GCR, but the relationship—if any—to local colonic CORT is unclear. Early life is also a critical developmental window for the gut microbiota, which is also impacted by ELS.[47–50] For example, we recently observed differences in microbiota composition between NR and MSEW mice characterized by lower abundance of a number of short chain fatty acid (SCFA)-producing taxa,[50] which may explain the delayed emergence of regulatory IL-10-producing CD4 T cells observed in 4-week-old MSEW mice. The second model employed in this study involved maternal ingestion of Dex, which could also potentially alter both the microbiota and the brain physiology of the pups. Interestingly, despite the very different approaches, we observed similar GC-related phenotypes in both models before and after induction of inflammation, suggesting that both regimens caused similar microbial changes or that the net effect of any microbial differences is minimal relative to the effects of reduced colonic CORT synthesis.

In summary, our study demonstrates how exposure to chronic stress during early life can lead to defective gut immune regulation, including inadequate colonic CORT production. Throughout our study, we observed that several, albeit statistically significant, ELS-dependent phenotypes and outcomes were not particularly dramatic relative to those of the control counterparts. Instead, the overarching effects of ELS appear to be cumulative and synergistic with additional colitogenic perturbations and served to exacerbate the effects of inflammation. Our findings are consistent with the multifactorial nature of IBD and demonstrate how this specific environmental trigger can contribute to worse disease outcomes in susceptible individuals (Figure 5).

Supplementary Data

Supplementary data is available at *Inflammatory Bowel Diseases* online.

Figure S1. Chronic colitis induces increased colonic Foxp3-, IL-10-, and IFNγ-, and IL-17A-expressing CD4 T cell populations independent of ELS. A, Representative flow cytometry plots showing Foxp3 and Thy1.1 expression by live CD4 T cells in the colons of PBS vehicle control and anti-IL-10R treated NR and MSEW mice at 8 weeks of age, 15 days after the last anti-IL-10R injection. B-C, Graphs summarizing frequencies (upper) and numbers (lower) of live CD4$^+$Foxp3$^+$(B) and live CD4$^+$Thy1.1$^+$ (C; $n \geq 8$). D, Representative flow cytometry plots showing IFNγ and IL-17A expression by live CD4 T cells in the colons of PBS vehicle control and anti-IL-10R treated NR and MSEW mice at 8 weeks of age, 15 days after the last anti-IL-10R injection. E-F, Frequency (upper) and numbers (lower) of live IFNγ$^+$CD4$^+$T cells (E) and live IL-17A$^+$CD4$^+$T cells (F; $n \geq 4$). Error bars represent mean ± SEM. Asterisks denote significance from 2-way ANOVA (B, C, E, F) followed by Tukey's multiple comparisons test at *$P < .05$, **$P < .01$, ***$P < .001$, and ****$P < .0001$. Data are compiled from 2-3 independent experiments.

Figure S2. MSEW does not lead differential induction of Il6, Il1b, or Tnf when mice are subjected to colitis. Relative mRNA levels of (A) *Il6*, (B) *Il1b*, and (C) *Nos2* in proximal colons of α-IL-10R–treated NR and MSEW mice normalized to PBS-treated NR mice ($n \geq 7$). All transcripts were initially normalized to *Tbp*. Error bars represent mean ± SEM. Asterisks denote significant differences from Brown-Forsythe and Welch ANOVA followed by Dunnett's T3 multiple comparisons test (A-C) at *$P < .05$, **$P < .01$, ***$P < .001$, and ****$P < .0001$.

Figure S3. Elevated induction of *Tnf* by nonepithelial cells in colitic MSEW mice relative to NR counterparts. A, Relative *Tnf* mRNA levels from epithelial cells (left) or epithelial-depleted colonic tissue (right) of α-IL-10R treated NR and MSEW male mice at Day 20, normalized to PBS-treated NR mice ($n \geq 3$). All transcripts were initially normalized to TATA box binding protein (*Tbp*). B, Representative flow cytometry plots showing TNF expression by live CD4 T cells in the colons of PBS treated NR and anti-IL-10R treated NR and MSEW mice on day 20. C, Frequency (left), number (middle), and mean fluorescent intensity (MFI, right) of live TNF$^+$CD4$^+$T cells ($n \geq 3$). Asterisks denote significance from 1-way ANOVA (A) followed by Tukey's multiple comparisons test at *$P < .05$, **$P < .01$, ***$P < .001$, and ****$P < .0001$.

Figure S4. Dex does not significantly impact *Il6* or *Il1b* induction or responsiveness when mice are subjected to colitis. Relative mRNA levels of (A) *Il6*, (B) *Il1b*, (C) *Il6ra*, (D) *Il1r1*, and (E) *Nos2* in proximal colon tissue (A, B, E) or crypt-enriched epithelial cells from the colons (C, D) of α-IL-10R–treated Veh and Dex mice, normalized to PBS-treated Veh mice ($n \geq 4$). All transcripts were initially normalized to *Tbp*. Error bars represent mean ± SEM. Asterisks denote significant

differences from Brown-Forsythe and Welch ANOVA followed by Dunnett's T3 multiple comparisons test (A, B, E) or 1-way ANOVA followed by Tukey's multiple comparisons test (C, D) at *$P < .05$, **$P < .01$, ***$P < .001$, and ****$P < .0001$.

Table S1. Primer sequences.

Author Contributions

R.Q.M., R.G.L., J.S.P., and C.L.M. conceived and designed research. C.L.M. supervised research. R.Q.M. performed all experiments with assistance from B.J.K., M.S.J., P.A.M., J.S.H., and C.E.K. J.B.F. performed colitis scoring. G.L. helped with interpretation of histological images and generated photomicrographs. R.Q.M. and C.L.M. wrote the manuscript.

Funding

Conflicts of Interest

R.G.L. is a current employee of Genentech, a member of the Roche group, and may hold Roche stock or stock options. All other authors declare that they have no competing financial interests.

References

1 Singh UP, Singh NP, Murphy EA, et al. Chemokine and cytokine levels in inflammatory bowel disease patients. *Cytokine.* 2016;77:44-49. doi:10.1016/j.cyto.2015.10.008

2 Adegbola SO, Sahnan K, Warusavitarne J, Hart A, Tozer P. Anti-TNF therapy in Crohn's disease. *Int J Mol Sci* . 2018;19(8):2244.

3 Vulliemoz M, Brand S, Juillerat P, Mottet C, Ben-Horin S, Michetti P. TNF-alpha blockers in inflammatory bowel diseases: practical recommendations and a user's guide: an update. *Digestion.* 2020;101(suppl 1):16-26. doi:10.1159/000506898

4 Brzozowski B, Mazur-Bialy A, Pajdo R, et al. Mechanisms by which stress affects the experimental and clinical inflammatory bowel disease (IBD): role of brain-gut axis. *Curr Neuropharmacol.* 2016;14(8):892-900. doi:10.2174/1570159x14666160404124127

5 Mawdsley JE, Rampton DS. Psychological stress in IBD: new insights into pathogenic and therapeutic implications. *Gut.* 2005;54(10):1481-1491. doi:10.1136/gut.2005.064261

6 Sun Y, Li L, Xie R, et al. Stress triggers flare of inflammatory bowel disease in children and adults. *Front Pediatr.* 2019;7:432-432. doi:10.3389/fped.2019.00432

7 Wu JC. psychological co-morbidity in functional gastrointestinal disorders: epidemiology, mechanisms and management. *J Neurogastroenterol Motil* 2012;18(1):13-18. doi:10.5056/jnm.2012.18.1.13

8 Merrick MTF, Derek C, Ports KA. *Vital Signs: Estimated Proportion of Adult Health Problems Attributable to Adverse Childhood Experiences and Implications for Prevention — 25 States, 2015–2017,* 2019. https://www.cdc.gov/mmwr/volumes/68/wr/mm6844e1.htm?s_cid=mm6844e1_w#suggestedcitation. Accessed 15 January 2023.

9 Juruena MF, Bourne M, Young AH, Cleare AJ. Hypothalamic-pituitary-adrenal axis dysfunction by early life stress. *Neurosci Lett.* 2021;759:136037. doi:10.1016/j.neulet.2021.136037

10 van Bodegom M, Homberg JR, Henckens MJAG. Modulation of the hypothalamic-pituitary-adrenal axis by early life stress exposure. *Front Cell Neurosci.* 2017;11:87-87. doi:10.3389/fncel.2017.00087

11 Sapolsky RM, Romero LM, Munck AU. How do glucocorticoids influence stress responses? integrating permissive, suppressive, stimulatory, and preparative actions*. *Endocr Rev.* 2000;21(1):55-89. doi:10.1210/edrv.21.1.0389

12 Korte SM, Koolhaas JM, Wingfield JC, McEwen BS. The Darwinian concept of stress: benefits of allostasis and costs of allostatic load and the trade-offs in health and disease. *Neuroscience & Biobehavioral Reviews* 2005;29(1):3-38. doi:10.1016/j.neubiorev.2004.08.009

13 Vegiopoulos A, Herzig S. Glucocorticoids, metabolism and metabolic diseases. *Mol Cell Endocrinol.* 2007;275(1):43-61. doi:10.1016/j.mce.2007.05.015

14 Vandevyver S, Dejager L, Libert C. Comprehensive overview of the structure and regulation of the glucocorticoid receptor. *Endocr Rev.* 2014;35(4):671-693. doi:10.1210/er.2014-1010

15 Talabér G, Jondal M, Okret S. Extra-adrenal glucocorticoid synthesis: immune regulation and aspects on local organ homeostasis. *Mol Cell Endocrinol.* 2013;380(1):89-98. doi:10.1016/j.mce.2013.05.007

16 Mueller M, Cima I, Noti M, et al. The nuclear receptor LRH-1 critically regulates extra-adrenal glucocorticoid synthesis in the intestine. *J Exp Med.* 2006;203(9):2057-2062. doi:10.1084/jem.20060357

17 Boivin MA, Ye D, Kennedy JC, et al. Mechanism of glucocorticoid regulation of the intestinal tight junction barrier. *Am J Physiol Gastrointest Liver Physiol.* 2007;292(2):G590-G598. doi:10.1152/ajpgi.00252.2006

18 Fischer A, Gluth M, Weege F, et al. Glucocorticoids regulate barrier function and claudin expression in intestinal epithelial cells via MKP-1. *Am J Physiol Gastrointest Liver Physiol.* 2013;306(3):G218-G228. doi:10.1152/ajpgi.00095.2013

19 Uellendahl-Werth F, Maj C, Borisov O, et al. Cross-tissue transcriptome-wide association studies identify susceptibility genes shared between schizophrenia and inflammatory bowel disease. *Commun Biol.* 2022;5(1):80. doi:10.1038/s42003-022-03031-6

20 Coste A, Dubuquoy L, Barnouin R, et al. LRH-1-mediated glucocorticoid synthesis in enterocytes protects against inflammatory bowel disease. *Proc Natl Acad Sci USA.* 2007;104(32):13098-13103. doi:10.1073/pnas.0702440104

21 Bruscoli S, Febo M, Riccardi C, Migliorati G. Glucocorticoid therapy in inflammatory bowel disease: mechanisms and clinical practice. *Front Immunol.* 2021;12:691480-691480. doi:10.3389/fimmu.2021.691480

22 Mays SG, Flynn AR, Cornelison JL, et al. Development of the first low nanomolar liver receptor homolog-1 agonist through structure-guided design. *J Med Chem.* 2019;62(24):11022-11034. doi:10.1021/acs.jmedchem.9b00753

23 Ho DH, Burch ML, Musall B, et al. Early life stress in male mice induces superoxide production and endothelial dysfunction in adulthood. *Am J Physiol Heart Circ Physiol.* 2016;310(9):H1267-H1274. doi:10.1152/ajpheart.00016.2016

24 George ED, Bordner KA, Elwafi HM, Simen AA. Maternal separation with early weaning: a novel mouse model of early life neglect. *BMC Neurosci.* 2010;11:123-123. doi:10.1186/1471-2202-11-123

25 Feng T, Wang L, Schoeb TR, Elson CO, Cong Y. Microbiota innate stimulation is a prerequisite for T cell spontaneous proliferation and induction of experimental colitis. *J Exp Med.* 2010;207(6):1321-1332. doi:10.1084/jem.20092253

26 He F. BCA (bicinchoninic acid) protein assay. *Bio-protocol* 2011;1(5):e44. doi:10.21769/BioProtoc.44

27 Maynard CL, Harrington LE, Janowski KM, et al. Regulatory T cells expressing interleukin 10 develop from Foxp3+ and Foxp3- precursor cells in the absence of interleukin 10. *Nat Immunol.* 2007;8(9):931-941. doi:10.1038/ni1504

28 Pohl CS, Medland JE, Moeser AJ. Early-life stress origins of gastrointestinal disease: animal models, intestinal pathophysiology, and translational implications. *Am J Physiol Gastrointest Liver Physiol.* 2015;309(12):G927-G941. doi:10.1152/ajpgi.00206.2015

29 Daskalakis NP, Claessens SE, Laboyrie JJ, et al. The newborn rat's stress system readily habituates to repeated and prolonged maternal separation, while continuing to respond to stressors in context dependent fashion. *Horm Behav.* 2011;60(2):165-176. doi:10.1016/j.yhbeh.2011.04.003

30 Enthoven L, Oitzl MS, Koning N, van der Mark M, de Kloet ER. Hypothalamic-pituitary-adrenal axis activity of newborn mice rapidly desensitizes to repeated maternal absence but becomes highly responsive to novelty. *Endocrinology.* 2008;149(12):6366-6377. doi:10.1210/en.2008-0238

31 Hong JY, Lim J, Carvalho F, et al. Long-term programming of CD8 t cell immunity by perinatal exposure to glucocorticoids. *Cell.* 2020;180(5):847-861.e15. doi:10.1016/j.cell.2020.02.018

32 Noti M, Corazza N, Tuffin G, Schoonjans K, Brunner T. Lipopolysaccharide induces intestinal glucocorticoid synthesis in a TNFα-dependent manner. *FASEB J.* 2010;24(5):1340-1346. doi:10.1096/fj.09-140913

33 Barreau F, Ferrier L, Fioramonti J, Bueno L. Neonatal maternal deprivation triggers long term alterations in colonic epithelial barrier and mucosal immunity in rats. *Gut.* 2004;53(4):501-506. doi:10.1136/gut.2003.024174

34 Hu CH, Xiao K, Luan ZS, Song J. Early weaning increases intestinal permeability, alters expression of cytokine and tight junction proteins, and activates mitogen-activated protein kinases in pigs. *J Anim Sci.* 2013;91(3):1094-1101. doi:10.2527/jas.2012-5796

35 Li B, Lee C, Zani A, et al. Early maternal separation induces alterations of colonic epithelial permeability and morphology. *Pediatr Surg Int.* 2014;30(12):1217-1222. doi:10.1007/s00383-014-3611-x

36 Smith F, Clark JE, Overman BL, et al. Early weaning stress impairs development of mucosal barrier function in the porcine intestine. *Am J Physiol Gastrointest Liver Physiol.* 2010;298(3):G352-G363. doi:10.1152/ajpgi.00081.2009

37 Faravelli C, Lo Sauro C, Godini L, et al. Childhood stressful events, HPA axis and anxiety disorders. *World J Psychiatry* 2012;2(1):13-25. doi:10.5498/wjp.v2.i1.13

38 Wu Y, Patchev AV, Daniel G, Almeida OFX, Spengler D. Early-life stress reduces dna methylation of the Pomc gene in male mice. *Endocrinology.* 2014;155(5):1751-1762. doi:10.1210/en.2013-1868

39 Bunea IM, Szentágotai-Tătar A, Miu AC. Early-life adversity and cortisol response to social stress: a meta-analysis. *Transl Psychiatry.* 2017;7(12):1274. doi:10.1038/s41398-017-0032-3

40 Perry RE, Rincon-Cortes M, Braren SH, et al. Corticosterone administration targeting a hypo-reactive HPA axis rescues a socially-avoidant phenotype in scarcity-adversity reared rats. *Dev Cogn Neurosci* 2019;40:100716. doi:10.1016/j.dcn.2019.100716

41 Young ES, Doom JR, Farrell AK, et al. Life stress and cortisol reactivity: an exploratory analysis of the effects of stress exposure across life on HPA-axis functioning. *Dev Psychopathol.* 2021;33(1):301-312. doi:10.1017/S0954579419001779

42 Smillie CS, Biton M, Ordovas-Montanes J, et al. Intra- and inter-cellular rewiring of the human colon during ulcerative colitis. *Cell.* 2019;178(3):714-730.e22. doi:10.1016/j.cell.2019.06.029

43 Noti M, Corazza N, Mueller C, Berger B, Brunner T. TNF suppresses acute intestinal inflammation by inducing local glucocorticoid synthesis. *J Exp Med.* 2010;207(5):1057-1066. doi:10.1084/jem.20090849

44 Huang S-C, Lee C-T, Chung B-C. Tumor necrosis factor suppresses NR5A2 activity and intestinal glucocorticoid synthesis to sustain chronic colitis. *Sci Signaling.* 2014;7(314):ra20-ra20. doi:10.1126/scisignal.2004786

45 Rahman MF, McGowan PO. Cell-type-specific epigenetic effects of early life stress on the brain. *Transl Psychiatry.* 2022;12(1):326. doi:10.1038/s41398-022-02076-9

46 Zannas AS, Chrousos GP. Epigenetic programming by stress and glucocorticoids along the human lifespan. *Mol Psychiatry.* 2017;22(5):640-646. doi:10.1038/mp.2017.35

47 Bailey MT, Coe CL. Maternal separation disrupts the integrity of the intestinal microflora in infant rhesus monkeys. *Dev Psychobiol.* 1999;35(2):146-155.

48 Callaghan BL, Fields A, Gee DG, et al. Mind and gut: associations between mood and gastrointestinal distress in children exposed to adversity. *Dev Psychopathol.* 2020;32(1):309-328. doi:10.1017/s0954579419000087

49 De Palma G, Blennerhassett P, Lu J, et al. Microbiota and host determinants of behavioural phenotype in maternally separated mice. *Nat Commun.* 2015;6:7735. doi:10.1038/ncomms8735

50 Kemp KM, Colson J, Lorenz RG, Maynard CL, Pollock JS. Early life stress in mice alters gut microbiota independent of maternal microbiota inheritance. *Am J Physiol Regul Integr Comp Physiol.* 2021;320(5):R663-R674. doi:10.1152/ajpregu.00072.2020